

f-Block Hydrides

Reversible Formation of a Cerium-Bound Terminal Hydride:
 $\text{Ce}(\text{C}_5\text{Me}_4\text{SiMe}_3)_2(\text{H})(\text{thf})$ Owen T. Summerscales,^[a] Enrique R. Batista,^[b] Brian L. Scott,^[c] Marianne P. Wilkerson,^[a] and Andrew D. Sutton^{*[a]}

Abstract: The use of the bulky cyclopentadienyl ligand Cp' ($\text{Cp}' = \text{C}_5\text{Me}_4\text{SiMe}_3$) to stabilize cerium hydrides has resulted in the preparation of two novel tuck-in complexes with C–H activated SiMe_3 groups. Subsequent reaction of these with H_2 in thf gives a lanthanide terminal hydride species $\text{Ce}(\text{Cp}')_2(\text{H})(\text{thf})$ which reversibly regenerates the tuck-in complex under sus-

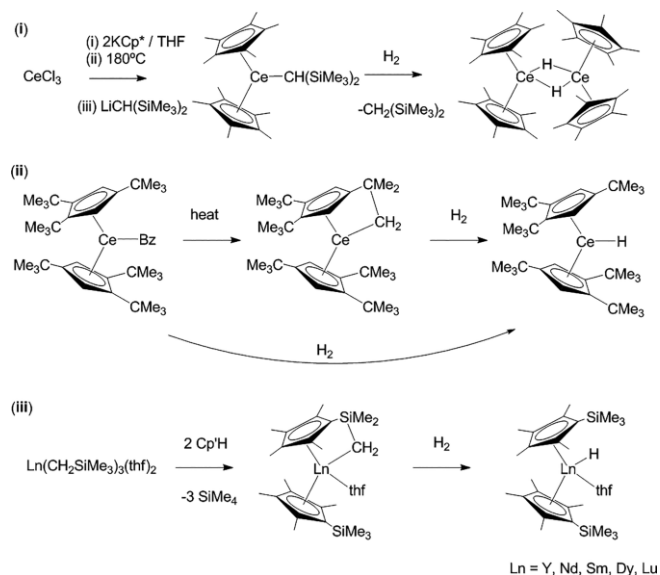
tained vacuum. This compound is only the second structurally characterized terminal cerium hydride. This new hydride is a catalyst in H/D exchange reactions between with both $\text{sp}^3\text{-CH}$ and $\text{sp}^2\text{-CH}$ bonds, and for the hydrogenation of unsaturated alkene bonds.

Introduction

Metal hydride complexes are important species in catalysis and continue to demand much attention for their complex reactivity patterns.^[1] In particular, lanthanide hydrides are among the most reactive coordination compounds known.^[2] However, their high reactivity is also associated with low stability – relatively few well-characterized lanthanide terminal hydride species are currently known.^[2–9]

We are particularly interested in the chemistry of cerium–hydrogen bonds: the one cerium species currently known containing a terminally-bound hydride (see right)^[3] has shown remarkable reactivity towards the breaking of internal and external C–H and C–F bonds (i.e. bonds found in both internal ligands and added external substrates).^[4] Highly Lewis-acidic, large lanthanide metal centers create a tendency for hydride species to dimerize, or oligomerize – this propensity is particularly noted for cerium. As the second-largest lanthanide trivalent ion, it is essential to use sterically-demanding ligands to prevent oligomerization. Cyclopentadienyl ligands have been shown in a few cases to stabilize isolable bridging and terminal cerium hydrides: the synthesis of a bridging hydride was first reported in the Cp^* complex $\{\text{Ce}(\text{C}_5\text{Me}_5)_2\text{H}\}_2$ by Teuben and co-workers,^[5] and similarly Bulchev et al. followed with $\{\text{Ce}(\text{C}_5\text{H}_3\text{tBu}_2)_2\text{H}\}_2$ in 1992.^[6] Lappert et al. reported a dimeric

metallocene salt with a bridging monohydride $\{[\text{Ce}(\text{C}_5\text{H}_4\text{SiMe}_2\text{tBu})_3]_2\text{-(H)}\}^+$,^[7] and a non-metallocene bridged dihydride cluster has also been recently reported by Okuda et al. $\{[\text{Ce}(\text{Me}_3\text{TACD})(\mu\text{-H})_2]_4; (\text{Me}_3\text{TACD})\text{H} = 1,4,7\text{-trimethyl-1,4,7,10-tetraazacyclo-dodecane, Me}_3[12\text{-aneN}_4]\}$.^[8] The only known terminal cerium hydride, $\text{Ce}(\text{C}_5\text{H}_2\text{tBu}_3)_2\text{H}$, was reported by Andersen et al. in 2005 (Scheme 1).^[3,4]



Scheme 1. Synthetic routes to previously known cerium and lanthanide hydride complexes.^[3,5,9]

The bulky Cp' ($\text{Cp}' = \text{C}_5\text{Me}_4\text{SiMe}_3$) ligand meanwhile shows promise for stabilizing a new type of cerium terminal hydride complex, and we have recently utilized the bis-substituted version of this ligand to stabilize the first structurally characterized bis-cyclopentadiene Ce^{IV} complex.^[10] Hou et al. have also used this ligand to effectively stabilize terminal lanthanide hydride complexes of the type $\text{Ln}(\text{Cp}')_2(\text{H})(\text{thf})$ ($\text{Ln} = \text{Y, Nd, Sm, Dy}$ and

[a] Chemistry Division, Los Alamos National Laboratory, Los Alamos, NM 87545, USA
E-mail: adsutton@lanl.gov
<http://www.lanl.gov/org/padste/adcles/chemistry/inorganic-isotope-actinide/chemical-energy-storage/index.php>

[b] Theoretical Division, Los Alamos National Laboratory, Los Alamos, NM 87545, USA

[c] Materials and Physics Applications Division, Los Alamos National Laboratory, Los Alamos, NM 87545, USA

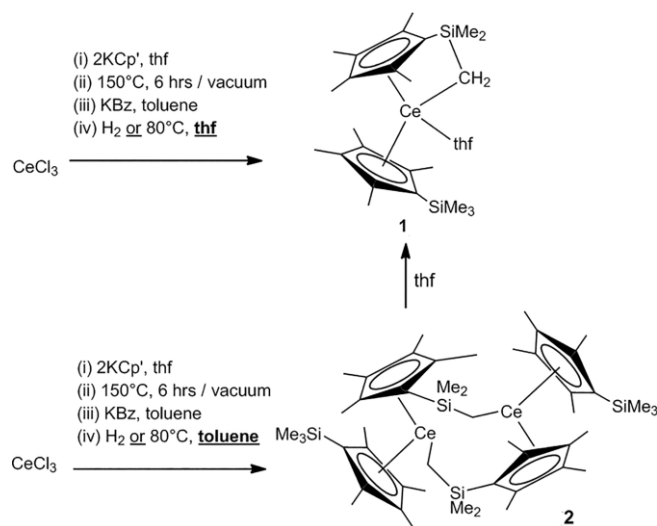
Supporting information and ORCID(s) from the author(s) for this article are available on the WWW under <http://dx.doi.org/10.1002/ejic.201600737>.

Lu, see Scheme 1),^[9] but did not report the cerium member of this series, presumably because their synthetic route could not be applied to this metal center, owing to the instability of the analogous starting material.

Here, we have successfully synthesized and structurally characterized a new Ce terminal hydride based on this series.

Results and Discussion

Hydrogenolysis of alkyl complexes has proven to be a successful strategy for synthesizing lanthanide hydrides (Scheme 1). The syntheses of $\text{Ln}(\text{Cp}')_2(\text{H})(\text{thf})$ use $\text{Ln}(\text{CH}_2\text{SiMe}_3)_3(\text{thf})_2$ as the starting material^[9] – however, for cerium, this complex has not been synthesized as a stable, fully characterizable compound. Therefore, we developed an alternative pathway to $(\eta^5:\eta^1\text{-C}_5\text{Me}_4\text{SiMe}_2\text{CH}_2)\text{Ce}(\text{Cp}')(\text{thf})$ (**1**) as a precursor for hydride formation. Sequential reaction of CeCl_3 with two equivalents of KCp' and one equivalent of KBz ($\text{Bz} = \text{benzyl}, \text{CH}_2\text{-Ph}$) gave a red crystalline material that when heated or reacted with H_2 generated the new tuck-in C–H activated complex $(\eta^5:\eta^1\text{-C}_5\text{Me}_4\text{SiMe}_2\text{CH}_2)\text{Ce}(\text{Cp}')(\text{thf})$ (**1**) as a crystalline solid in low yield (19 % from CeCl_3 ; Scheme 2).



Scheme 2. Formation of **1** and **2** from CeCl_3 .

Crystalline samples of **1** gave reproducible fingerprint ^1H and $^{13}\text{C}\{^1\text{H}\}$ NMR spectra, with paramagnetically broadened and highly shifted resonances, which could not be unambiguously assigned. Variable temperature (VT) NMR measurements [–50 to 100 °C (dec.), d_8 -toluene] showed a complex pattern of coalescence and subsequent decoalescence of the spectra and failed to enable full assignment (see supporting information).

Primary characterization of **1** was obtained via single crystal X-ray diffraction, as for most of the other members of the series previously reported,^[9] using a single crystal grown from hexane at –30 °C. The structure was solved in triclinic space group $P\bar{1}$, and shows a monomeric sandwich complex with one internally C–H activated SiMe_3 group forming a metallacycle with the $\text{C}_5\text{Me}_4\text{SiMe}_2\text{CH}_2$ ligand (Figure 1). Ce–C distances are typical for this type of complex (Table 1).^[3] This structure is analogous to $(\eta^5:\eta^1\text{-C}_5\text{Me}_4\text{SiMe}_2\text{CH}_2)\text{Ln}(\text{Cp}')(\text{thf})$ ($\text{Ln} = \text{Y}, \text{Nd}, \text{Sm}, \text{Dy}$ and

Lu),^[9] and similar to a cyclometalated sandwich complex reported by Andersen et al. (Scheme 1).^[3]

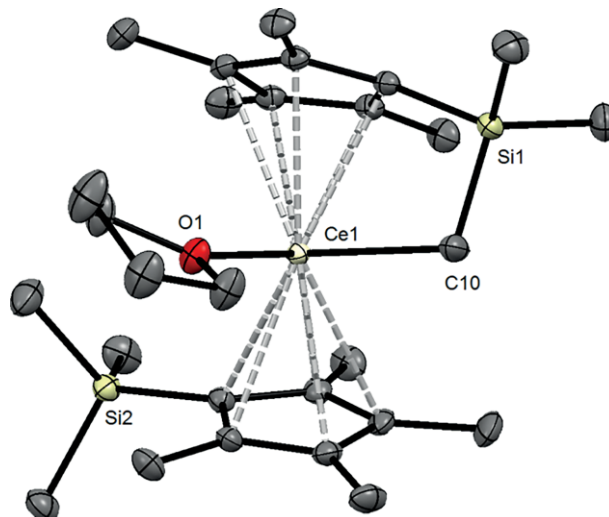


Figure 1. Thermal ellipsoid plot of the structure of **1** (hydrogen atoms omitted; ellipsoids at 50 % probability).

Table 1. Selected bond lengths and angles for complexes **1** and **2**.

Bond lengths [Å]			
1		2	
Ce(1)–O(1)	2.5207(11)	Ce(1)–C(22)	2.746(3)
Ce(1)–C(10)	2.5790(15)	Ce(1)–C(Cp') av.	2.8262(19)
Ce(1)–C(Cp') av.	2.8167(14)	Ce(1)–C(13)	2.819(2)
Ce(1)–C(1)	2.7016(15)	Ce(1)–C(14)	2.868(2)
Ce(1)–C(2)	2.7877(13)	Ce(1)–C(15)	2.8399(19)
Ce(1)–C(3)	2.8772(13)	Ce(1)–C(16)	2.7996(19)
Ce(1)–C(4)	2.8363(13)	Ce(1)–C(17)	2.7643(18)
Ce(1)–C(5)	2.7252(13)		
Bond angles [°]			
1		2	
Si(1)–C(10)–Ce(1)	97.91(6)	Si(2)–C(22)–Ce(1)'	150.77(12)
C(5)–C(1)–Si(1)	125.51(11)	C(17)–C(16)–Si(2)	124.29(15)
C(2)–C(1)–Si(1)	123.89(11)	C(15)–C(16)–Si(2)	128.72(15)
C(10)–Si(1)–C(1)	102.32(7)	C(22)–Si(2)–C(16)	112.19(11)

Hydrogenation of the red crystalline material obtained from the Cp'/KBz reaction in toluene (as a non-coordinating solvent, rather than thf) gave a new species, identified as $\{(\text{Cp}')\text{Ce}(\mu\text{-}\eta^5:\eta^1\text{-C}_5\text{Me}_4\text{SiMe}_2\text{CH}_2)_2\}$ (**2**) in 17 % yield from CeCl_3 (Scheme 2). Complex **2** crystallized in orthorhombic space group $Pcan$; the structure shows a dimeric sandwich species containing one intact Cp' ligand and one cyclometalated ligand, similar to that found in **1**, but as a “tuck-over” bridging ligand between two cerium centers (Figure 2).

The complex forms an asymmetric bridging structure, with the cyclometalated ligands found adjacent to one another, presumably due to crystal packing forces. Ce–C distances are typical for this type of complex (Table 1).^[3,11] VT NMR (–50 to 100 °C) of concentrated solutions of crystalline material showed only residual protio solvent resonance in the ^1H and $^{13}\text{C}\{^1\text{H}\}$ NMR spectra. Presumably this is because of severe paramagnetic broadening similar to other 4f-element complexes.

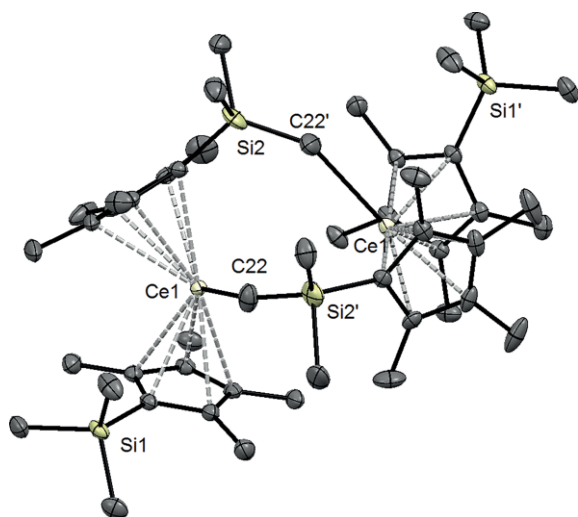
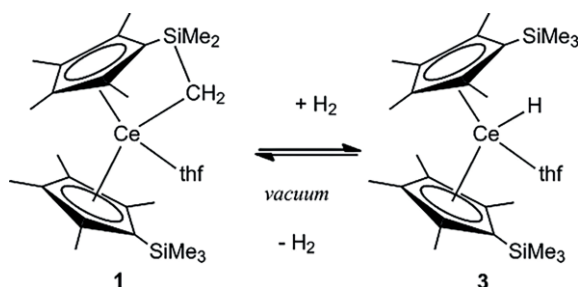


Figure 2. Thermal ellipsoid plot of the structure of **2** (hydrogen atoms omitted; ellipsoids at 50 % probability).

Addition of thf to **2** results in thf coordination and monomer formation to give **1** as evidenced by ^1H NMR spectroscopy (Scheme 2). Complexes analogous to **1** will react with H_2 to form terminal hydrides (Scheme 1).^[9] For the smaller lanthanides Y, Dy and Lu the reaction was irreversible, however for the larger metals Nd and Sm, the process was found to be reversible under the application of vacuum (Scheme 3).



Scheme 3. Formation of **3** from **1**.

We find that when **1** is exposed to H_2 (1 atm) in situ, new peaks are observed in the ^1H NMR spectrum of **1** (C_6D_6 ; $\delta = 79.6, 13.2$ ppm), although no noticeable color change is observed. Some peaks of any new hydride product may be missing due to paramagnetic broadening, or due to CH/CD scrambling with the solvent (see below). These new peaks disappear after taking the solution to dryness and holding under vacuum for 30 min, but reappear when H_2 is added back to the NMR tube indicating a reversible process on addition or removal of H_2 .

The ^2H NMR spectrum of the reaction between **1** and D_2 in (protio) toluene gave two broadened resonances at $\delta = -0.38$ and -6.71 ppm, which were presumably owing to a deuterated ligand bound to cerium, in addition to a more distinct set of resonances for d_8 -toluene. Resonances for both the aromatic and aliphatic C–H groups of the toluene were observed. This data indicate that both sp^2 - and sp^3 -C–H activation of the solvent is occurring, presumably via exchange at the Ce–H moiety. This behavior has been documented previously for analogous

bis-cyclopentadienyl lanthanide alkyl and hydride complexes, e.g. for $\{\text{Cp}^*_2\text{M}(\text{H})(\text{thf})\}_x$ ($\text{M} = \text{Y}, \text{Sc}$).^[12–14] In the latter cases, a monomeric (terminal) hydride is speculated as the active species,^[13] although never directly isolated. An identical ^2H NMR experiment performed using thf also showed sp^3 -C–H/D scrambling; in this case the 2,5-CH bonds were, on average, exchanged five times more than the 3,4-CH bonds, as determined by the relative integration of the peaks.

Recrystallization of **1** under a H_2 atmosphere resulted in the new crystallographically characterized terminal hydride species $\text{Ce}(\text{Cp}')_2(\text{H})(\text{thf})$ (**3**). The structure of **3** was solved in monoclinic $P 2_1/n$ and shows a sandwich complex, with intact SiMe_3 groups, isostructural to the series described previously (Figure 3).^[9] The terminal hydride could be located and isotropically refined, giving a Ce–H distance of 2.264(4) Å (Table 2), significantly longer than the Ce–H bond found in $\text{Ce}(\text{C}_5\text{H}_2\text{tBu}_3)_2\text{H}$ [1.90(5) Å],^[3] the only previously known cerium terminal hydride. Bridging cerium hydrides meanwhile have been reported in the range 2.327–2.678 Å.^[6–8] Presumably, the longer bond is due to a more congested steric environment at the cerium center in **3**. Although crystals of **3** could be obtained, elemental analysis data was not reliable as solid samples of the compound slowly revert back to **3** when the H_2 atmosphere is removed or rapidly when under vacuum.

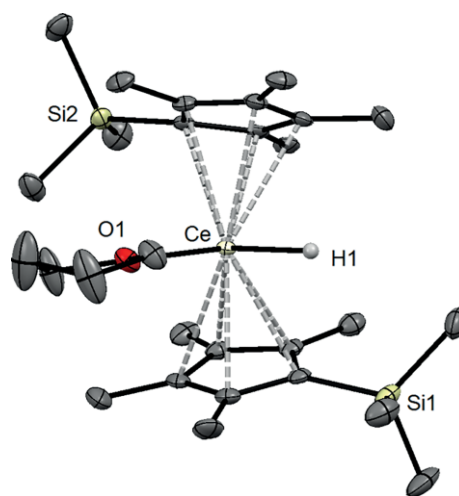


Figure 3. Thermal ellipsoid plot of the structure of **3** (H atoms omitted; ellipsoids at 50 % probability).

Table 2. Selected bond lengths and angles for complex **3**.

Bond lengths [Å]		Bond angles [°]	
Ce(1)–H(1)	2.264(4)	C(1)–Si(1)–C(10)	110.34(8)
Ce(1)–O(1)	2.530(4)	C(1)–Si(1)–C(11)	112.2(3)
Ce(1)–C(Cp')		C(1)–Si(1)–C(12)	110.34(8)
av. (C1–5)	2.779(5)		
Ce(1)–C(Cp')			
av. (C13–17)	2.797(5)		

Addition of H_2 to **2** meanwhile produced no change in the ^1H NMR spectrum (C_6D_6). Crystals were again grown under an atmosphere of H_2 and gave the same unit cell as **2**, i.e. no reaction was observed.

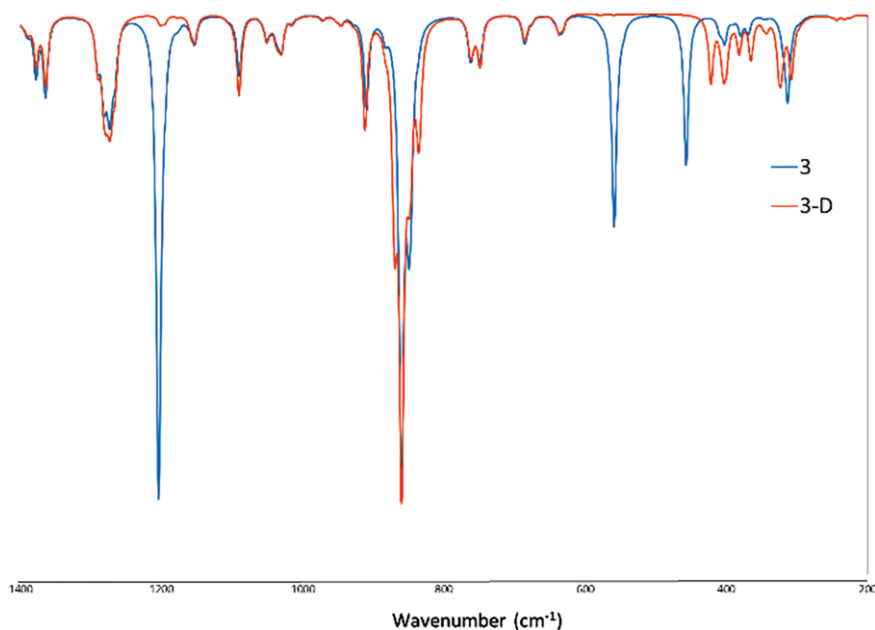


Figure 4. Calculated IR spectra of **3** and **3-D**.

The values for cerium–hydrogen bond stretches in the infrared spectrum for $\text{Ce}(\text{C}_5\text{H}_2\text{tBu}_3)_2\text{H}$ could not be assigned by Andersen et al.^[3] Likewise, Hou et al. did not report the identification of any Ln–H stretches for $\text{Ln}(\text{Cp}^*)_2(\text{H})(\text{thf})$ (Ln = Y, Nd, Sm, Dy and Lu).^[9]

Comparison of the IR spectrum of **3** with a sample prepared using D_2 (**3-D**) did not show any obvious peaks that could be expected for Ce–H or Ce–D vibrational resonances: the Ln–H (Ln = lanthanide) absorption is known to be located in the 1100–1350 cm^{-1} range for bridging hydrides [e.g. $(\text{Cp}^*\text{LnH})_2$]^[2,12] but which is often obscured by bands attributed to metal-bound thf^[2] (terminal transition metal hydride bonds are meanwhile observed in the region of 1600 to 2250 cm^{-1}).^[11]

In order to guide us in peak assignment, we used density functional calculations to predict the frequency of the Ce–H stretching mode. **3** was first optimized in gas phase and very good agreement between the experimental and optimized structures was obtained for the metal ligand distances, e.g. Ce–thf 2.557 Å (1 % error), and Ce–Cp'(centroid) 2.529 and 2.505 Å (0.1 and 0.2 % error). The Ce–H distance optimized to 2.135 Å, which is 6 % shorter than the experimental value, which we believe is due to our model not taking into account an interaction with a thf molecule on an adjacent molecule. Scanning of the Ce–H potential energy including a second molecule (albeit constrained at the crystal structure) yields a minimum at 2.28 Å, which is in close agreement with experiment. However, for calculation of vibrational modes one needs to be at a potential energy minimum which forces us to use the optimized structure with Ce–H at 2.135 Å, and accepting an error in the absolute frequency. From the calculated spectrum, the Ce–H mode is clearly identified as the normal mode at 1213 cm^{-1} (Figure 4). The transverse modes of the Ce–H couple with the ligand bending modes, which leads to a broader band at low frequencies in the range between 350 and 600 cm^{-1} .

Two main normal modes, at 478 and 598 cm^{-1} , were seen as the most dominated by the Ce–H vibration modes. Replacing hydride for deuteride shifts the vibrational frequency by the change in effective mass i.e. square root of 2. The new stretching mode is therefore calculated at 876 cm^{-1} . The low frequency bend band also moves to lower frequencies of 332 and 438 cm^{-1} . We observe a strong absorption centered around 800 cm^{-1} in the spectra of both **3** and **3-D**, possibly due to the bound thf, which apparently obscures this new Ce–D peak in **3-D** (see Supporting Information).

Given the unique reversibility of the formation of the hydride, we were curious to test for possible olefin hydrogenation reactivity, which is well-known for a variety of metal hydride species.^[11] Initial ^1H NMR (C_6D_6) screening showed that **1** was a functional pre-catalyst for the hydrogenation of *cis*-stilbene, *tert*-butylethylene and styrene (ambient temperatures and pressures, 5 % catalyst). This behavior would be expected for cyclopentadienyl lanthanide hydrides, which have known as hydrogenation catalysts since the 1980s, when they were amongst the most active known at the time.^[15] In this case, we demonstrate that in solution, the hydride functionality is accessible and active, likely part of an equilibrium between cyclometalated **1** and hydride **3**.

Conclusions

3 is the second known example of a terminal cerium hydride complex, which has proved challenging to synthesize and necessitated a different preparative route than reported for the analogues based on Y, Nd, Sm, Dy and Lu.^[9] In the same manner, we obtained a cyclometalated “tuck-in” species **1** as a precursor to the hydride **3**, however isolation of synthetic intermediates to **1** (e.g. the presumed benzyl compound) was not possi-

ble. The dimeric “tuck-over” analog **2** was obtained by exclusion of thf; such “tuck-in” and “tuck-over” complexes are common amongst f-element metallocenes.^[16] The new terminal hydride species **3** reversibly reforms the cyclometalated parent species **1** upon prolonged exposure to vacuum. This behavior, which is notably different from the Andersen hydride $\text{Ce}(\text{C}_5\text{H}_2\text{fBu}_3)_2\text{H}$ (which forms the hydride from the cyclometalated precursor irreversibly^[3]), is likely to indicate a unique reactivity profile of **3** towards external substrates. Indeed, we have found that **3** facilitates C–H/D exchange between D_2 and benzene, toluene or thf, catalytically. We currently are exploring more reactivity modes of this compound.

Experimental Section

General: Unless noted otherwise, all operations were performed under a purified argon atmosphere in a standard MBraun UniLab drybox or under an argon atmosphere using high-vacuum and Schlenk techniques. Hydrocarbon solvents were purchased anhydrous from Sigma–Aldrich, and further dried with activated molecular sieves (4 Å). Deuterated solvents were purchased from Cambridge Isotope Laboratory, and dried with molecular sieves (4 Å). Unless noted, chemicals were purchased from commercial sources and used without further purification. $\text{K}(\text{CH}_2\text{C}_6\text{H}_5)$ was prepared by deprotonation of toluene by $\text{KOtBu}/n\text{BuLi}$. $\text{K}(\text{C}_5\text{Me}_4\text{SiMe}_3)$ was prepared by deprotonation of $\text{C}_5\text{Me}_4(\text{H})\text{SiMe}_3$ by $\text{K}[\text{N}(\text{SiMe}_3)_2]$ in toluene. $\text{C}_5\text{Me}_4(\text{H})\text{SiMe}_3$, $\text{K}[\text{N}(\text{SiMe}_3)_2]$, $n\text{BuLi}$ (1.6 M in hexanes) and KOtBu were purchased from Sigma–Aldrich and used as received. H_2 gas was provided by the LANL in-house gas facility at 99.9 % grade. CeCl_3 was purchased anhydrous from Strem and used as received. All NMR spectra were recorded using a Bruker 400 Ultra Shield spectrometer. ^1H NMR spectra were referenced to solvent residual peaks ($\delta = 7.15$ ppm for C_6D_6). Infrared spectra were measured as KBr discs using a Perkin–Elmer Spectrum Two FTIR spectrometer. Elemental analyses were performed by Midwest Microlab (Indianapolis, IN).

$(\eta^5\text{-}\eta^1\text{-C}_5\text{Me}_4\text{SiMe}_2\text{CH}_2)\text{Ce}(\text{C}_5\text{Me}_4\text{SiMe}_3)(\text{thf})$ (1**):** A mixture of CeCl_3 (0.392 g, 1.59 mmol) and $\text{K}(\text{C}_5\text{Me}_4\text{SiMe}_3)$ (0.74 g, 3.18 mmol) were stirred in thf (50 mL) overnight, resulting in the formation of a yellow solution. Filtration through celite and removal of volatiles gave a bright yellow solid, assumed to be “ $\text{Ce}(\text{C}_5\text{Me}_4\text{SiMe}_3)_2\text{-Cl}_2\text{K}(\text{thf})_x$ ”, which was subsequently de-solvated at 150 °C for 6 h under vacuum ($m = 0.828$ g). This process resulted in a subtle color change from bright- to straw-yellow. This material [assumed to be “ $\text{Ce}(\text{C}_5\text{Me}_4\text{SiMe}_3)_2\text{Cl}_2\text{K}$ ”], was combined with $\text{K}(\text{CH}_2\text{C}_6\text{H}_5)$ (0.169 g, 1.30 mmol) in toluene and stirred overnight to yield a green solution. This was filtered through celite, leaving yellow solids, and then reduced to dryness in vacuo. The solids were subsequently extracted into hexane (50 mL) and filtered again through celite. The subsequent green-red dichroic solution was reduced in volume to 10 mL and a dark red crystalline material was obtained after cooling to –30 °C. Finally, this material was re-dissolved in thf (20 mL) and hydrogen (1 atm) was added to the degassed solution with stirring, whereupon the green color turned to pink. After stirring for 30 min, the solvent was removed by vacuum and the product recrystallized from a minimum quantity of hexane at –30 °C ($m = 0.069$ g, 0.12 mmol, 17 % yield from CeCl_3). ^1H NMR (C_6D_6): $\delta = 18.75$ (br.), 11.37 (br.), 8.44 (br.), 6.45 (br.), 2.13 (br.), –0.46 (br.), –2.66 (br.), –5.05

(br.), –6.98 (br., two peaks overlapping), –13.69 (s, br.), –23.27 (br.), –33.97 (br.) ppm. $^{13}\text{C}\{^1\text{H}\}$ NMR (C_6D_6): $\delta = 4.6, 6.4, 11.6, 13.8, 14.3, 23.0, 32.0, 242.3$ (* some peaks not observed presumably due to paramagnetism) ppm. ^1H NMR (d_8 -toluene): $\delta = 18.45$ (br.), 11.14 (br.), 8.27 (br.), 6.30 (br.), 2.16 (br.), –0.49 (br.), –2.61 (br.), –5.09 (br.), –7.51 (br., two peaks overlapping), –13.74 (br.), –22.91 (br.), –34.49 (br.) ppm. ^1H NMR ($[\text{D}_8]\text{thf}$): $\delta = 19.70$ (br.), 12.02 (br.), 9.38 (br.), 7.11 (br.), 4.97 (br.), 3.80 (br.), 0.46 (br.), –0.58 (br.), –3.11 (br.), –5.65 (br.), –11.98 (br.), –32.76 (br.), –33.65 (br., two peaks overlapping) ppm. Elemental analysis for $\text{C}_{24}\text{H}_{41}\text{CeSi}_2$ (**1** – thf) calcd. % (found) C 54.82 (54.47) H 7.86 (7.89). IR (KBr disc): $\tilde{\nu} = 2723$ (w), 2139 (w), 1571 (w), 1445 (br., s), 1382 (m), 1323 (s), 1245 (s), 1188 (w), 1124 (m), 1020 (s), 951 (w), 921 (w), 837 (br., s), 753 (s), 679 (s), 628 (s), 565 (w) cm^{-1} .

$\{(\text{C}_5\text{Me}_4\text{SiMe}_3)\text{Ce}(\mu\text{-}\eta^5\text{-}\eta^1\text{-C}_5\text{Me}_4\text{SiMe}_2\text{CH}_2)\}_2$ (2**). Method 1:** Hydrogenolysis. Hydrogen (1 atm) was added to a degassed solution of **1** (0.100 g, 0.16 mmol) in toluene (20 mL) with stirring, whereupon the green color immediately turned to pink. After stirring for 30 min, the solvent was removed by vacuum and the product recrystallized from a minimum quantity of hexane at –30 °C ($m = 0.056$ g, 0.05 mmol, 67 % yield). ^1H and $^{13}\text{C}\{^1\text{H}\}$ NMR (C_6D_6): no observable signals. Elemental analysis for $\text{C}_{48}\text{H}_{82}\text{Ce}_2\text{Si}_4$ calcd. % (found) C 53.81 (53.37) H 7.86 (7.95). IR (KBr disc): $\tilde{\nu} = 1621$ (br., w), 1441 (m), 1326 (m), 1248 (s), 1026 (s), 942 (s), 837 (s), 753 (m), 687 (w), 629 (w), 628 (w), 553 (w) cm^{-1} .

Method 2: Thermolysis. A solution of **1** (0.100 g, 0.16 mmol) in hexane (20 mL) was heated to 60 °C in a sealed ampule with a Teflon® stopcock for one hour, whereupon the green color turned to pink. the solvent was removed by vacuum and the product recrystallized from a minimum quantity of hexane at –30 °C ($m = 0.060$ g, 0.06 mmol, 72 % yield).

$\text{Ce}(\text{C}_5\text{Me}_4\text{SiMe}_3)_2(\text{H})(\text{thf})$ (3**):** A sample of **1** was exposed to H_2 (1 atm; no color change observed) which formed **3** quantitatively by ^1H NMR spectroscopy. **3** could be recrystallized under a H_2 atmosphere (hexane) however was not stable as a solid due to loss of H_2 and formation of **1** under vacuum. ^1H NMR (C_6D_6): $\delta = 80.2$ (s, br.), 19.14 (s, br.), 11.66 (s, br.), 8.61 (s, br.), 6.51 (s, br.), –3.07 (s, br.), –5.44 (s, br.), –7.43 (s, br.), –8.16 (s, br.), –14.15 (s, br.), –23.88 to –24.83 (m, br.), –35.01 to –36.79 (m, br.) ppm. $^{13}\text{C}\{^1\text{H}\}$ NMR (C_6D_6): $\delta = 4.6, 6.4, 11.6, 13.8, 14.3, 23.0, 32.0, 242.3$ ppm (* some peaks not observed presumably due to paramagnetism).

Computational Methodology: The calculations of minimum-energy geometries, vibrational modes and frequencies, and infrared spectra of all of the compounds in this paper were computed at the density functional theory level, using the hybrid functional from the Truhlar group M06.^[17] The Ce ion was represented by the SDD pseudopotential^[18] whereas for the light elements all-electron basis sets were employed. The C, O, and Si centers were represented by Pople’s 6-31+g* basis set. The smaller 6-31g was used for all the hydrogen atoms as they are removed from the metal center. One exception was made for the hydride center where we used the larger 6-311+g* basis set in an effort to best describe the electronic structure of the region of interest. All the calculations were carried out with the Gaussian09 rev. D.01 package.^[19]

CCDC 1056189 (for **1**), 1056190 (for **2**), and 1056191 (for **3**) contain the supplementary crystallographic data for this paper. These data can be obtained free of charge from The Cambridge Crystallographic Data Centre.

Supporting Information: Crystallographic tables cif files for **1–3**, experimental procedures and characterizing data for **1–3**.

Acknowledgments

This work was funded by Los Alamos National Laboratory LDRD-DR (Laboratory Directed Research and Development – Directed Research). Los Alamos National Laboratory is operated by Los Alamos National Security, LLC, for the National Nuclear Security Administration of the U.S. Department of Energy under contract DE-AC5206NA25396.

Keywords: Hydrides · C–H activation · Lanthanides · Cerium

- [1] H. D. Kaesz, R. B. Saillant, *Chem. Rev.* **1972**, 72, 231.
- [2] D. Barbier-Baudry, A. Dormond, in: *Recent Advances in Hydride Chemistry* (Eds.: M. Peruzzini, R. Poli), Elsevier Science **2002**, p. 249–270.
- [3] L. Maron, E. L. Werkema, L. Perrin, O. Eisenstein, R. A. Andersen, *J. Am. Chem. Soc.* **2005**, 127, 279.
- [4] a) E. L. Werkema, E. Messines, L. Perrin, L. Maron, O. Eisenstein, R. A. Andersen, *J. Am. Chem. Soc.* **2005**, 127, 7781; b) E. L. Werkema, L. Maron, O. Eisenstein, R. A. Andersen, *J. Am. Chem. Soc.* **2007**, 129, 2529; c) E. L. Werkema, R. A. Andersen, *J. Am. Chem. Soc.* **2008**, 130, 7153; d) E. L. Werkema, A. Yahia, L. Maron, O. Eisenstein, R. A. Andersen, *Organometallics* **2010**, 29, 5103; e) E. L. Werkema, A. Yahia, L. Maron, O. Eisenstein, R. A. Andersen, *New J. Chem.* **2010**, 34, 2189; f) E. L. Werkema, L. Castro, L. Maron, O. Eisenstein, R. A. Andersen, *Organometallics* **2012**, 31, 870; g) L. Perrin, E. L. Werkema, O. Eisenstein, R. A. Andersen, *Inorg. Chem.* **2014**, 53, 6361.
- [5] H. J. Heeres, J. Renkema, M. Booi, A. Meetsma, J. H. Teuben, *Organometallics* **1988**, 7, 2495.
- [6] Y. K. Gun'ko, B. M. Bulychev, G. L. Soloveichik, V. K. Belsky, *J. Organomet. Chem.* **1992**, 424, 289.
- [7] Y. K. Gun'ko, P. B. Hitchcock, M. F. Lappert, *Organometallics* **2000**, 19, 2832.
- [8] D. Martin, J. Kleemann, E. Abinet, T. P. Spaniol, L. Maron, J. Okuda, *Eur. J. Inorg. Chem.* **2013**, 3987.
- [9] Y. Takenaka, Z. Hou, *Organometallics* **2009**, 28, 5196.
- [10] A. D. Sutton, D. L. Clark, B. L. Scott, J. C. Gordon, *Inorganics* **2015**, 3, 589.
- [11] M. Booi, A. Meetsma, J. H. Teuben, *Organometallics* **1991**, 10, 3246.
- [12] W. J. Evans, J. H. Meadows, A. L. Wayda, W. E. Hunter, J. L. Atwood, *J. Am. Chem. Soc.* **1982**, 104, 2008.
- [13] M. Booi, B. J. Deelman, R. Duchateau, D. S. Postma, A. Meetsma, J. H. Teuben, *Organometallics* **1993**, 12, 3531.
- [14] M. E. Thompson, S. M. Baxter, A. R. Bulls, B. J. Burger, M. C. Nolan, B. D. Santarsiero, W. P. Schaefer, J. E. Bercaw, *J. Am. Chem. Soc.* **1987**, 109, 203.
- [15] G. A. Molander, E. D. Dowdy, *Top. Organomet. Chem.* **1999**, 2, 119.
- [16] K. R. D. Johnson, P. G. Hayes, *Chem. Soc. Rev.* **2013**, 42, 1947.
- [17] Y. Zhao, D. G. Truhlar, *Theor. Chem. Acc.* **2008**, 120, 215.
- [18] A. Bergner, M. Dolg, W. Kuechle, H. Stoll, H. Preuss, *Mol. Phys.* **1993**, 80, 1431.
- [19] M. J. Frisch, G. W. Trucks, H. B. Schlegel, G. E. Scuseria, M. A. Robb, J. R. Cheeseman, G. Scalmani, V. Barone, B. Mennucci, G. A. Petersson, H. Nakatsuji, M. Caricato, X. Li, H. P. Hratchian, A. F. Izmaylov, J. Bloino, G. Zheng, J. L. Sonnenberg, M. Hada, M. Ehara, K. Toyota, R. Fukuda, J. Hasegawa, M. Ishida, T. Nakajima, Y. Honda, O. Kitao, H. Nakai, T. Vreven, J. A. Montgomery Jr., J. E. Peralta, F. Ogliaro, M. Bearpark, J. J. Heyd, E. Brothers, K. N. Kudin, V. N. Staroverov, R. Kobayashi, J. Normand, K. Raghavachari, A. Rendell, J. C. Burant, S. S. Iyengar, J. Tomasi, M. Cossi, N. Rega, J. M. Millam, M. Klene, J. E. Knox, J. B. Cross, V. Bakken, C. Adamo, J. Jaramillo, R. Gomperts, R. E. Stratmann, O. Yazyev, A. J. Austin, R. Cammi, C. Pomelli, J. W. Ochterski, R. L. Martin, K. Morokuma, V. G. Zakrzewski, G. A. Voth, P. Salvador, J. J. Dannenberg, S. Dapprich, A. D. Daniels, Ö. Farkas, J. B. Foresman, J. V. Ortiz, J. Cioslowski, D. J. Fox, *Gaussian 09*, revision D.01, Gaussian, Inc., Wallingford CT, **2013**.

Received: June 20, 2016

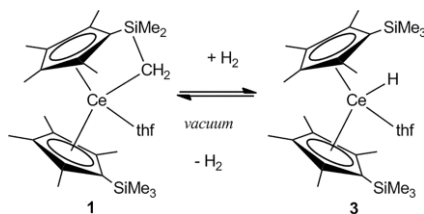
Published Online: ■

f-Block Hydrides

O. T. Summerscales, E. R. Batista,
B. L. Scott, M. P. Wilkerson,
A. D. Sutton* 1–7



Reversible Formation of a Cerium-Bound Terminal Hydride: $\text{Ce}(\text{C}_5\text{Me}_4\text{SiMe}_3)_2(\text{H})(\text{thf})$



The cerium tuck-in metallocene $\text{Ce}(\text{C}_5\text{H}_4\text{SiMe}_3)(\text{C}_5\text{H}_4\text{SiMe}_2\text{CH}_2)(\text{thf})$ was synthesized and shown to reversibly form a terminal hydride species $\text{Ce}(\text{C}_5\text{H}_4\text{SiMe}_3)_2(\text{H})(\text{thf})$ upon reaction with H_2 . This new hydride is a catalyst in H/D exchange reactions between with both $\text{sp}^3\text{-CH}$ and $\text{sp}^2\text{-CH}$ bonds, and for the hydrogenation of unsaturated alkene bonds.

DOI: 10.1002/ejic.201600737